

Vibration Isolation using a Shunted Electromagnetic Transducer

S. Behrens, A. J. Fleming, S. O. R. Moheimani
School of Electrical Engineering and Computer Science
University of Newcastle NSW 2308 Australia

ABSTRACT

By attaching an electromagnetic transducer to a mechanical isolation system and shunting the terminals of the transducer with electrical impedance, we can provide improved isolation performance while eliminating the need for an additional sensor. Simulated and experimental results on a simple electro-mechanical isolation system show that the proposed controller is capable of peak damping and high frequency attenuation.

1. INTRODUCTION

An isolation system¹⁻³ attempts to mitigate the mass displacement x resulting from a base disturbance y . A low-frequency mass-spring-damper is often employed as a mechanical filter. Additional attenuation and control of the mechanical resonance can be achieved with a force generated by an electromagnetic transducer. A common application of an isolation system is an automobile suspension system.⁴ Most suspension systems are active^{3,5-10}, that is, they sense using an accelerometer, or a force transducer, and actuate using an electromagnetic transducer.

Electromagnetic transducers can be used as sensors, actuators or both.¹¹⁻¹⁶ A simple technique for both sensing and actuating of mechanical vibration control is known as *electromagnetic shunt damping*.¹⁷ By connecting an electrical impedance to the terminals of an electromagnetic coil, the relative mechanical velocity between the coil and magnet can be reduced. Electromagnetic shunt damping belongs to a broad field of research commonly referred to as *electromagnetic shunt control*.

For electromagnetic shunt control both the sensor and actuator are combined together as self-sensing.¹⁷ From a theoretical viewpoint, the control scheme is considered perfectly *collocated*,¹⁸ which improves the stability and robustness of the closed-loop system.

In this paper, we apply electromagnetic shunt control to a simple isolation system. The effect of the electromagnetic shunt control is studied theoretically and then validated experimentally on a simple electro-mechanical isolation system. This technique will be referred to as *electromagnetic shunt isolation*.

This paper consists of six sections. After this introduction, Section 2 will introduce background analysis for a simple mechanical isolation system. In Section 3, we discuss a method for modeling the presence of an electromagnetic shunt on a simple electro-mechanical isolation system. Section 4, proposes a passive control algorithm which consists of a series capacitor-resistor impedance. Then in Section 5, experimental results for a simple electromagnetic isolation apparatus are presented. Conclusions will be discussed in Section 6.

2. BACKGROUND

The concepts of *damping* and *isolation* of vibration are sometime confused. In a few words, *damping* is defined as the reduction of amplitude of the system within a limited bandwidth near the resonance frequency. While *isolation* is defined as supporting a static load within a particular bandwidth ω_c , and attenuation (or filtered) of high frequency components above ω_c , as shown in Figure 1.

Vibration isolation can be divided into two different categories. The two cases are: (1) isolated mass may contain a disturbance (normally a force) which propagates into the base structure, and (2) a disturbance generated by the base structure propagating into the isolated mass. The second case is found more commonly in the engineering environment, therefore, we will focus all our attention to this particular case.

Corresponding author: S. Behrens: E-mail: sbehrens@ecemail.newcastle.edu.au; Telephone: +61 2 4921 7223. Fax: +61 2 4921 7058. Support for this research has been provided by grants from Australian Research Council (ARC).

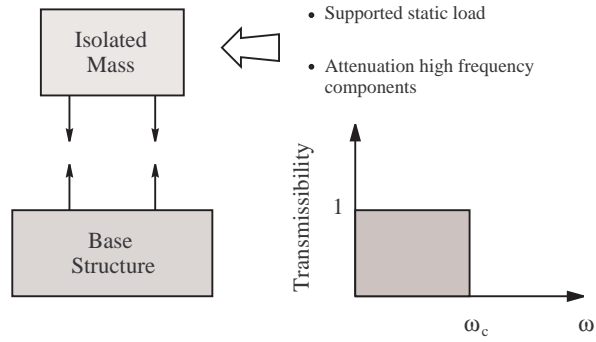


Figure 1. Principle of an isolation system and isolation objectives.

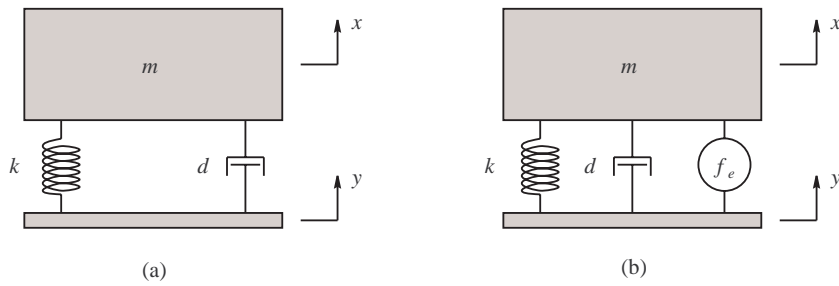


Figure 2. Simple mass spring damper isolation system: (a) unforced and (b) forced systems.

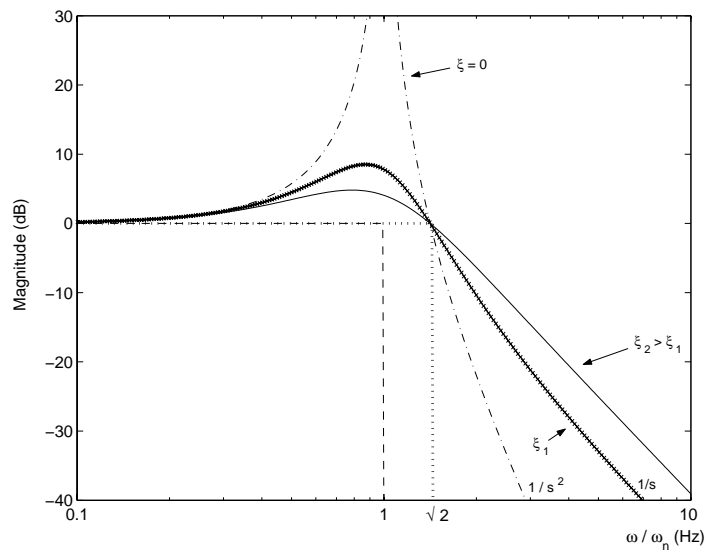


Figure 3. Normalized transmissibility ratio of a passive damper for various values of damping ratio ζ .

Consider the simple isolation system shown in Figure 2 (a). The isolation system consists of a linear spring in parallel with a passive damper, where m is the mass, k and d are the stiffness and damping coefficient respectively. The equation of motion is defined as

$$m\ddot{x}(t) + d\dot{x}(t) + kx(t) = d\dot{y}(t) + ky(t), \quad (1)$$

where $(\ddot{\cdot})$ and $(\dot{\cdot})$ denote the acceleration and velocity of $x(t)$ and $y(t)$. The resonance or cut-off frequency of the mechanical system is $\omega_n = \sqrt{\frac{k}{m}}$ and the amount of damping is defined by the damping ratio ζ where $\frac{d}{m} = 2\zeta\omega_n$. The transfer function in Laplace domain, between the disturbance displacement y and the mass displacement x is given by

$$T(s) \triangleq G_{yx}(s) = \frac{x(s)}{y(s)} = \frac{ds + k}{ms^2 + ds + k} = \frac{\frac{2\zeta s}{\omega_n} + 1}{\frac{s^2}{\omega_n^2} + \frac{2\zeta s}{\omega_n} + 1}. \quad (2)$$

Figure 3 shows a general plot for the *transmissibility ratio* $T(s)$ of Equation (2), where the ratio between the disturbing frequency and the resonant frequency ω_n . Many interesting observations can be learned from this transfer function:

1. When the disturbing frequency coincides with the natural frequency of the system, an overshoot appears showing that the system vibrates at this frequency with high amplitudes.
2. The frequency where the curve crosses over the 0 dB line is reached when the disturbing frequency is equal to $\omega_c = \sqrt{2}\omega_n$. This critical frequency is the point where the influence of vibration isolation begins.
3. At low frequencies, below the resonance of the system, the displacement of the sensitive payload follows faithfully the displacement of the disturbance source as if the isolator were infinitely rigid. However, at higher frequencies, greater than the resonance frequency of the system, the curve rolls-off and the displacement of the payload decreases gradually while the disturbance is constant.
4. When we increase the damping ratio ζ , the overshoot that appears at the natural frequency decreases but, unfortunately, the sharpness of the roll-off at high frequency decreases too.
5. To maintain the sharp roll-off at high frequency while decreasing the overshoot at the resonance, a control algorithm is needed.

For Figure 3, we can see that when $\zeta = 0$, the high frequency roll-off is $1/s^2$ (-40 dB/decade) while very large amplitude is seen near the natural frequency ω_n . On the other hand, when the damping ratio ζ is increased we reduce the overshoot at the resonance but we reduce also the roll-off to $1/s$ (-20 dB/decade). As a result, the design of a mechanical passive damper involves a trade-off between the resonance amplification and the high frequency attenuation.

3. MODELLING

3.1. Forced Isolation Problem

Consider a simple isolation system, as shown in Figure 2 (a), by taking the Laplace of Equation (1), we obtain the following transfer function relating the applied base velocity $w(s)$ and isolated mass velocity $v(s)$, that is

$$T(s) \triangleq G_{wv}(s) = \frac{v(s)}{w(s)} = \frac{ds + k}{ms^2 + ds + k}. \quad (3)$$

where $w(s) = s y(s)$ and $v(s) = s x(s)$. It should be noted, that $G_{wv}(s)$ is equivalent to the transmissibility ratio $T(s)$.

For the forced isolation problem, as shown in Figure 2 (b), a control force $f_e(t)$ is placed between the mass and the base. For this system, the equation of motion is

$$m\ddot{x}(t) + d\dot{x}(t) + kx(t) + f_e(t) = d\dot{y}(t) + ky(t). \quad (4)$$

By taking the Laplace of Equation (4), we obtain

$$v(s) = \frac{ds + k}{ms^2 + ds + k}w(s) - \frac{s}{ms^2 + ds + k}f_e(s), \quad (5)$$

where $w(s)$ and $f_e(s)$ are the inputs to the system.

3.2. Developing the Electromagnetic Shunt Isolation System

Consider, a shunted electromagnetic transducer, as shown in Figure 4. To determine the opposing force $f_e(s)$, we need to consider the simplified electrical model of the shunted electromagnetic transducer. Ohm's law states that

$$V_z(s) = I_z(s)Z(s), \quad (6)$$

where $V_z(s)$ is the voltage across the terminals of the shunt impedance $Z(s)$, and $I_z(s)$ is the corresponding current. According to Kirchhoff's voltage law, we obtain the following relationship between $V_e(s)$ and $V_z(s)$, as $V_z(s) = V_e(s) - (L_e s + R_e)V_z(s)$ which implies

$$V_z(s) = \frac{Z(s)}{Z(s) + L_e s + R_e} V_e(s). \quad (7)$$

For an ideal electromagnetic transducer, the voltage V_e is proportional to the relative velocity,^{17,19} that is

$$V_e(s) = c_{vv} (v(s) - w(s)), \quad (8)$$

where c_{vv} is the electro-mechanical coefficient relating relative velocity to voltage. By substituting, (8) into (7), we obtain

$$V_z(s) = \frac{Z(s)}{Z(s) + L_e s + R_e} c_{vv} (v(s) - w(s)). \quad (9)$$

Alternatively, the current flowing through the shunt $I_z(s)$, that is,

$$I_z(s) = \frac{V_z(s)}{Z(s)} = \frac{c_{vv}}{Z(s) + L_e s + R_e} (v(s) - w(s)), \quad (10)$$

and the opposing shunt force $f_e(s) = c_{if} I_z(s)$, assuming an ideal transducer, is

$$f_e(s) = \frac{c_{vv} c_{if}}{L_e s + R_e + Z(s)} (v(s) - w(s)). \quad (11)$$

Substituting (11) into (5), the electromagnetic shunt isolation system $w(s)$ to $v(s)$, is

$$\tilde{T}(s) \triangleq \tilde{G}_{wv}(s) = \frac{\left(d + \frac{c_{vv} c_{if}}{L_e s + R_e + Z(s)}\right) s + k}{ms^2 + \left(d + \frac{c_{vv} c_{if}}{L_e s + R_e + Z(s)}\right) s + k}. \quad (12)$$

The reader may note that the damped system $\tilde{G}_{wv}(s)$, or sometimes referred to as the closed-loop system, is equivalent to the damped transmissibility ratio $\tilde{T}(s)$.

4. CONTROLLER DESIGN

When a piezoelectric transducer is shunted by a passive electrical network, it acts as a medium for dissipating mechanical energy of the attached structure. Forward²¹ and Hagood *et. al.*²² suggested that a series inductor-resistor circuit attached across the conducting surfaces of a piezoelectric transducer can be tuned to dissipate mechanical energy of a host structure. They demonstrated the effectiveness of this technique by tuning the resulting inductor-resistor ($L - R$) and inherit capacitance of the piezoelectric transducer, to a specific resonance frequency of the host structure.

For electromagnetic shunt isolation, we can apply the same methodology as suggested above. For this particular system, though, we need to apply a series capacitor-resistor ($C - R$) as suggested by Behrens *et. al.*¹⁷ The shunt impedance is

$$Z(s) = \frac{1}{Cs} + R \quad (13)$$

where C is tuned to the resonance frequency of the mechanical structure,

$$C = \frac{1}{\omega_n^2 L_e} = \frac{1}{\frac{k}{m} L_e}. \quad (14)$$

In order to determine an optimal value for the shunt resistance R , an optimization approach could be considered. By minimizing the \mathcal{H}_2 norm of the closed-loop system $\tilde{T}(s)$, or $\tilde{G}_{wv}(s)$, we can determine the appropriate resistance value R .²⁰ This requires a solution to the following optimization problem to be found

$$R_t^* = \arg \min_{R_t > 0} \left\| \tilde{T}(s) \right\|_2 \quad (15)$$

where the total resistance R_t is equivalent to $R_t = R_e + R$.

Now, the electromagnetic shunt force is

$$\begin{aligned} f_e(s) &= \frac{c_{vv}c_{if}}{L_e s + R_e + Z_p(s)} (v(s) - w(s)) \\ &= \frac{c_{vv}c_{if}kL_e s}{kL_e^2 s^2 + kL_e R_t s + m} (v(s) - w(s)) \end{aligned} \quad (16)$$

and the composite electromagnetic shunt isolation system is

$$\begin{aligned} \tilde{T}(s) &\triangleq \frac{\left(d + \frac{c_{vv}c_{if}}{L_e s + R_e + Z(s)} \right) s + k}{ms^2 + \left(d + \frac{c_{vv}c_{if}}{L_e s + R_e + Z(s)} \right) s + k} \\ &= \frac{\left(d + \frac{c_{vv}c_{if}kL_e s}{kL_e^2 s^2 + kL_e R_t s + m} \right) s + k}{ms^2 + \left(d + \frac{c_{vv}c_{if}kL_e s}{kL_e^2 s^2 + kL_e R_t s + m} \right) s + k}. \end{aligned} \quad (17)$$

5. EXPERIMENTAL VALIDATION

5.1. Experimental Apparatus

To support the proposed isolation electromagnetic shunting technique experiments were carried out at the Laboratory for Dynamics and Control of Smart Structures (LDCSS)*. A photograph of the simple isolated electromagnetic apparatus, is shown in Figure 5. The apparatus consists of two identical Jaycar Electronics[†] subsonic transducer Cat. XC-1008. Each transducer consists of a permanent toroid magnet, a coil, supporting frame, magnetic circuit and flexible supports, as shown in Figure 6. Each transducer is mechanically equivalent to the electromagnetic mass spring damper shown in Figure 6.

By connecting two identical electromagnetic transducers together, as shown in Figure 7, where transducer 1 is the isolated mass spring damper system and transducer 2 as the base disturbance, we obtain a simple experimental isolation system. Note transducer 2 is connected to ground, for our case a Newport RS 3000 optical table was utilized.

Now, a disturbance current $I_d(s)$ is applied to the transducer 2 as a base disturbance, we can measure the transmissibility ratio $T(s)$ of the isolated mass. To measure the transmissibility ratio, two B&K accelerometer were used to measure the applied base velocity $w(s)$, accelerometer 2, and the isolated mass velocity $v(s)$, accelerometer 1, as shown in Figure 7. An experimental magnitude frequency response was obtained for transmissibility ratio i.e. $T(s) \triangleq G_{wv}(s)$, as shown in Figure 8.

To model the isolated system, the isolated mass m , damping constant d , spring constant k , coil inductance L_e , coil resistance R_e and the electro-mechanical coefficients c_{vv} and c_{if} need to be determined. The isolated mass, coil inductance and resistances can be measured directly, while damping and spring constant can be determined by using the resonance frequency of the isolated system i.e. ω_n can be obtained from Figure 8, $d = 2\zeta\omega_n m$ and $k = \omega_n^2 m$. To determine the electro-mechanical coefficients c_{vv} and c_{if} , a disturbance current $I_d(s)$ is applied to transducer 2. Assuming the electromagnetic transducer is linear for low frequencies and displacements, we can measure transducer 1 voltage and relative velocity of the isolation mass $v(s) - w(s)$. Experimental parameters for the isolated system are as listed in Table 1.

*School of Electrical Engineering & Computer Science, University of Newcastle, NSW, Australia.
<http://rumi.newcastle.edu.au/lab>

[†]www.jaycar.com.au

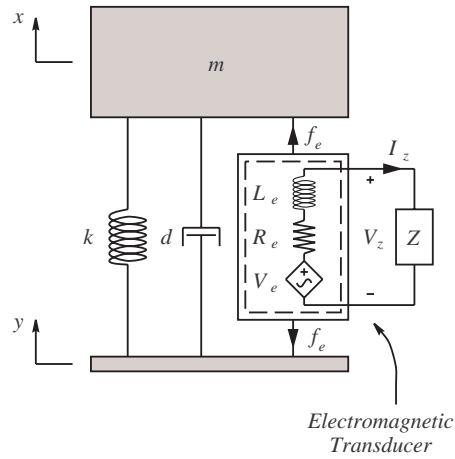


Figure 4. Electromagnetic shunted isolation system.

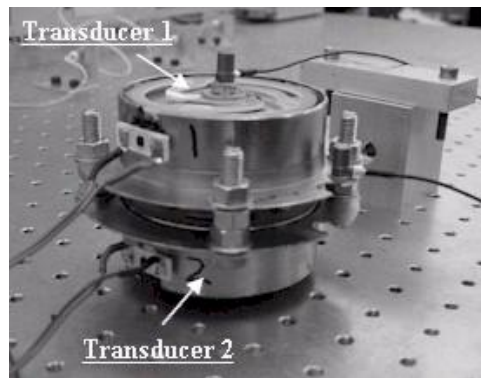


Figure 5. Isolation experimental apparatus. Note transducer 2 is used as a disturbance.

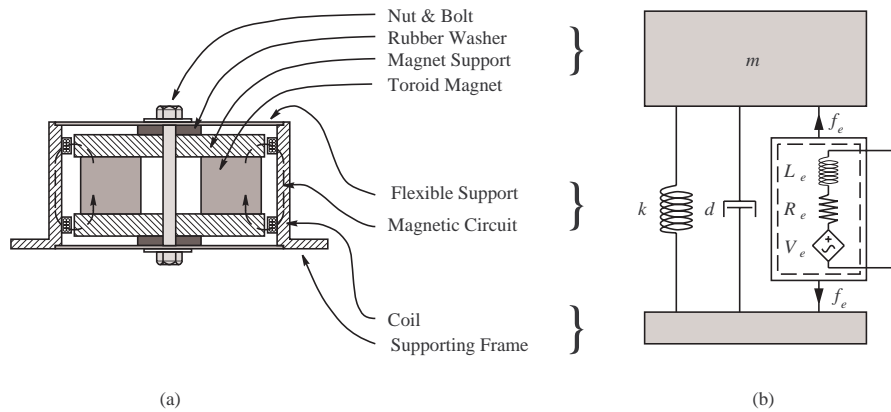


Figure 6. Electromagnetic transducer: (a) cross section, and (b) mechanical equivalent.

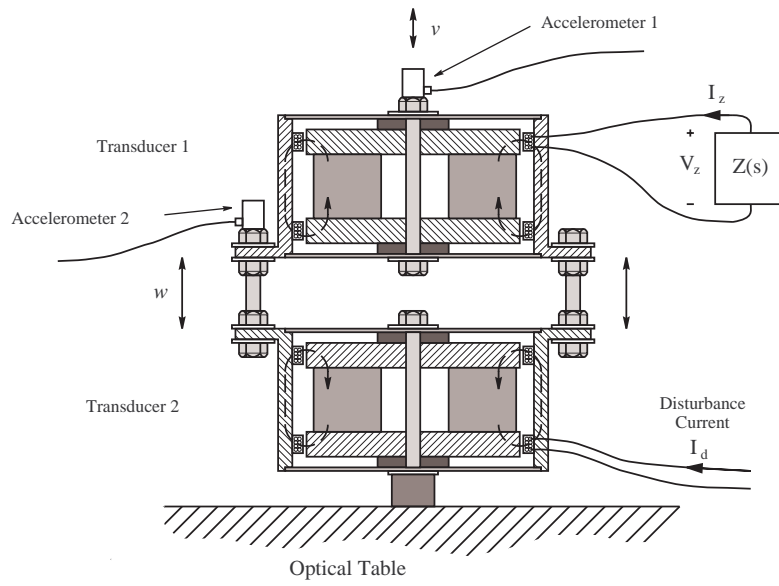


Figure 7. Sideview of the experimental isolation apparatus. Transducer 1 is shunted by electrical impedance (or admittance), while applying a base disturbance current $I_d(s)$ to transducer 2.

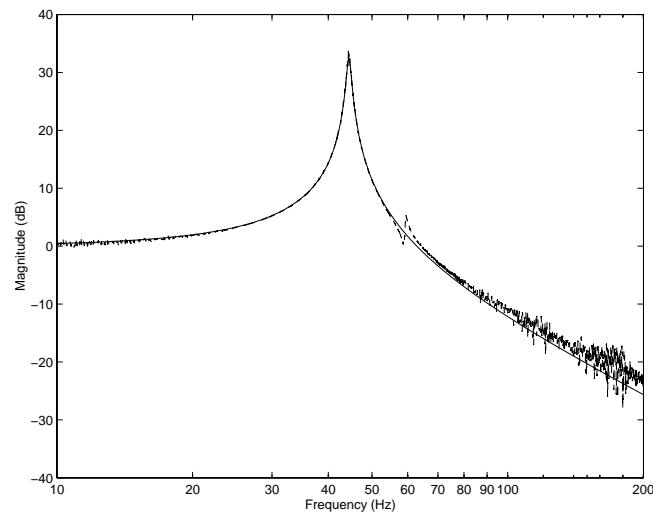


Figure 8. Transmissibility ratio $T(s)$: experimental (---) and simulated (—).

Parameter	Value
Isolated mass m	0.4 kg
Damping constant d	2.68 Nsm ⁻¹
Spring constant k	32 kNm ⁻¹
Electro-mechanical c_{vv} and c_{if}	3.36
Coil inductance L_e	0.323 mH
Coil resistance R_e	4.0 Ω

Table 1. Electromagnetic transducer parameters.

5.2. Implementation of Shunt Impedance

Referring to Figure 9, the terminal impedance of an arbitrary electrical network $Z_T(s)$ can be implemented by either: (a) measuring the terminal current i_z and controlling the terminal voltage v_z , or (b) measuring the terminal voltage v_z and controlling the terminal current i_z . The motivation and benefits behind such techniques are thoroughly discussed in reference Fleming *et. al.*²⁰

For the purpose of this paper, we will only consider the first case, a shown in Figure 9 (a). The controlled voltage v_z is set to be a function of the measured current i_z . i.e. $v_z = f(i_z)$. If the function $f(i_z)$, is a linear transfer function $Z(s)$ whose input is the measured current i_z , i.e. $V_z(s) = Z(s)I_z(s)$, then the terminal impedance $Z_T(s)$ is equal to $Z(s)$. This is termed a current-controlled-voltage-source (CCVS).

5.3. Simulated and Experimental Results

Using the experimental parameters, as in listed in Table 1, and the impedance

$$Z(s) = \frac{1}{0.0407s} - 3.87,$$

we can simulate the open- and closed-loop response as shown in Figure 10. From simulation, shown in Figure 10, the passive controller has considerably damped the resonance mode ≈ 28 dB.

Experiments were performed on the experimental apparatus using the current-controlled-voltage-source (CCVS), as described in Section 5.2. Experimental results for $G_{wv}(s)$ and $\tilde{G}_{wv}(s)$, or $T(s)$ and $\tilde{T}(s)$, frequency response are shown in Figure 11.

Simulation and experimental results concur, as shown in Figures 10 and 11. The reader may observe the cut-off frequency ω_c has shifted higher in frequency, that is, the open-loop cut-off frequency was $\omega_c = \sqrt{2}\omega_n = \frac{\sqrt{2}}{2\pi} \sqrt{\frac{k}{m}} = 63.3$ Hz and the closed-loop ω_c is approximately equal to 65 Hz. In addition, the closed-loop system has also retained -20 dB/decade high frequency attenuation.

Overall, this particular technique is very effective around the resonance, approximately 28 dB peak reduction. The control scheme also offers both static load support and high frequency attenuation. Further research into the area includes setting up the electromagnetic isolation problem as a standard feedback control problem; LQR , LQG , or \mathcal{H}_2 control problem. Similar work can be found in Fleming *et. al.*²³

6. CONCLUSION

In this paper, we have demonstrated an innovative vibration isolation device which provides peak and high frequency attenuation. By shunting an electromagnetic transducer, with impedance, we can eliminate the need for additional sensor. A simple experimental apparatus validated the proposed isolation control scheme.

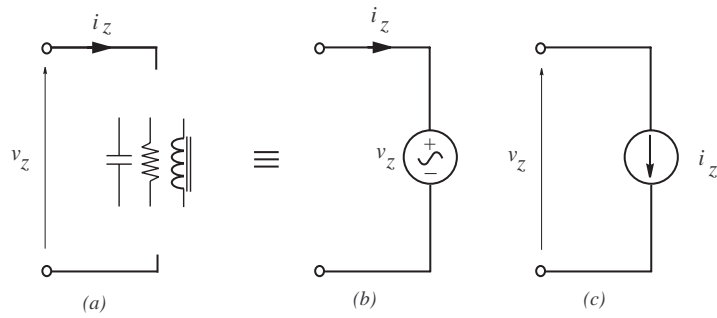


Figure 9. An arbitrary terminal impedance (a), a synthetic impedance (b), and a synthetic admittance (c).

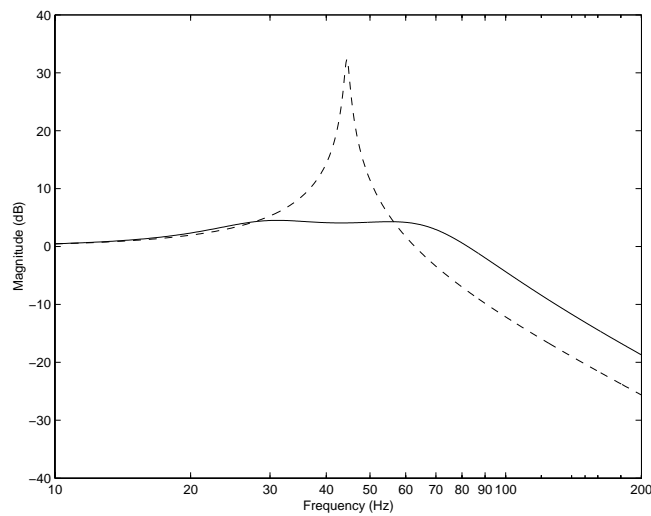


Figure 10. Simulated passive shunt $T(s)$ open- (---) and $\tilde{T}(s)$ closed-loop (—) frequency response.

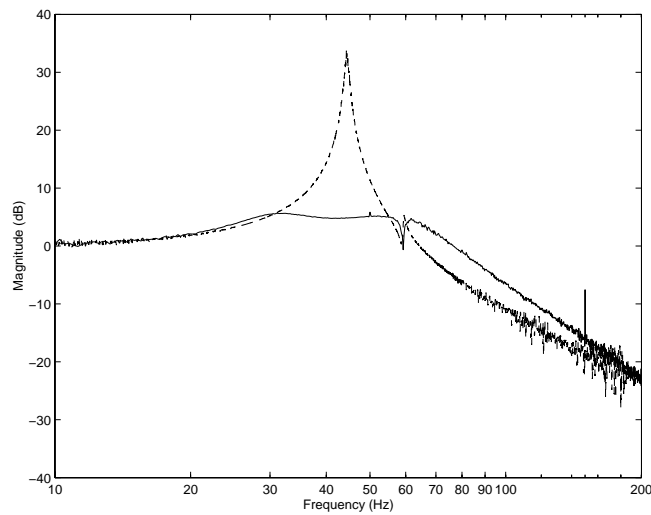


Figure 11. Experimental passive shunt $T(s)$ open- (---) and $\tilde{T}(s)$ closed-loop (—) frequency response.

REFERENCES

1. S. S. Rao. *Mechanical Vibrations*. Addison-Wesley Publishing Company, 3rd edition, 1995.
2. D. J. Inman. *Engineering Vibrations*. Prentice Hall, 2nd edition, 2000. ISBN: 013726142X.
3. C. H. Hansen and S. D. Hansen. *Active Control of Noise and Vibration*. Chaman & Hall, 1997. ISBN: 0419193901.
4. T. D. Gillespie, *Fundamentals of Vehicle Dynamics*, Society of Automotive Engineers, 1992.
5. J. W. Choi, Y. B. Seo, W. S. Yoo, and M. H. Lee, "Lqr approach using eignstructure assignment with an active suspension control application," in *Proc. IEEE International Conference on Control Applications*, pp. 1235–1239, (Trieste, Italy), September 1998.
6. H. C. Sohn, K. S. Hong, and J. K. Hedrick, "Semi-active control of the macpherson suspension system: Hardware-in-the-loop simulations," in *Proc. IEEE International Conference on Control Applications*, pp. 982–987, (Anchorage, Alaska USA), September 2000.
7. T. Fukao, A. Yamawaki, and N. Adachi, "Nonlinear and hinf control of active suspension systems with hydraulic actuators," in *Proc. IEEE Conference on Decision and Control*, pp. 5125–5128, (Phoenix, Arizona USA), December 1999.
8. D. S. Joo, N. Al-Holou, J. M. Weaver, Lahdhir, and F. Al-Abbas, "Nonlinear modeling of vehicle suspension systems," in *Proc. IEEE American Control Conference*, pp. 115–118, (Chicago, Illinois USA), June 2000.
9. S. Ikenaga, F. L. Lewis, J. Campos, and L. Davis, "Active suspension control of ground vehicle based on a full-vehicle model," in *Proc. IEEE American Control Conference*, pp. 4019–4024, (Chicago, Illinois USA), June 2000.
10. M. C. Smith and F. Wang, "Controlle parameterization for disturnbance response decoupling: Application to vehicle active suspension control," *IEEE Transactions on Control Systems Technology* **10**:393–407, May 2002.
11. S. Mirzaei, S. M. Saghaiannejad, V. Tahani, and M. Moallem. Linear electric actuators and generators. *IEEE Transaction on Energy Conversion*, **14**(3):712–717, September 1999.
12. B. M. Hanson, M. D. Brown, and J. Fisher. Self sensing: Closed-loop estimation for a linear electromagnetic actuator. In *Proc. IEEE American Control Conference*, pp. 1650–1655, Arlington, VA USA, June 2001.
13. Y. B. Kim, W. G. Hwang, C. D. Kee, and H. B. Yi. Active vibration control of suspension system using an electromagnetic damper. In *Proc. Of the Int. MECH Eng. Part D Journal of Automoblie Engineering*, **8**:865–873, 2001.
14. J. Shaw. Active vibration isolation by adaptive control. In *Proc. IEEE International Conference on Control Applications*, pp. 1509–1514, Hawaii, USA, August 1999.
15. D. Vischer and H. Bleuler. Self-sensing active magnetic levitation. *IEEE Transactions on Magnetics*, **29**(2):169–177, 1993.
16. N. Morse, R. Smith, B. Paden, and J. Antaki. Position sensed and self-sensing magnetic bearing configurations and associated robustness limitations. In *Proc. IEEE Conference on Decision and Control*, pp. 2599–2604, Tampa, Florida USA, December 1998.
17. S. Behrens, A. Fleming, and S. O. R. Moheimani, "Electromagnetic shunt damping," in *IEEE/ASME International Conference on Advanced Intelligent Mechatronics 2003*, (Kobe, Japan), July 2003.
18. D. G. MacMartin, "Collocated structural control: motivation and methodology," in *Proc. IEEE International Conference on Control Applications*, pp. 1092–1097, (Albany, New York USA), September 1995.
19. S. Behrens, A. Fleming, and S. O. R. Moheimani, "Electrodynamic vibration suppression," in *Proc. SPIE Smart Structures and Materials 2003 - Damping and Isolation, Paper No. 4697-24*, (San Diego, CA USA), December 2002.
20. A. J. Fleming, S. Behrens, and S. O. R. Moheimani, "Optimization and implementation of multi-mode piezoelectric shunt damping systems," *IEEE/ASME Transactions on Mechatronics* **7**:87–94, March 2002.
21. R. L. Forward, "Electronic damping of vibrations in optical structures," *Applied Optics* **18**:690–697, March 1979.
22. N. W. Hagood and A. Von Flotow, "Damping of structural vibrations with piezoelectric materials and passive electrical networks," *Journal of Sound and Vibration* **146**(2):243–268, 1991.
23. A. Fleming, S. Behrens, and S. O. R. Moheimani. Active \mathcal{H}_2 and \mathcal{H}_∞ shunt control of electromagnetic transducer. In *IEEE Conference on Decision and Control*, December 2003.